(Reprinted from Nature, Vol. 271, No. 5641, pp. 147–150, January 12, 1978)

Guinea Current upwelling

THE historical record of maritime observations are summarised here to indicate the dominant seasonal variations in upwelling, and in certain associated processes, within the Guinea Current region. The region is similar to other eastern ocean boundary upwelling areas in the appearance of cool sea temperatures near the coast, productive coastal fisheries, and a zone of low rainfall on the adjacent coast (Fig. 1). It differs from some of the more studied regions in several important respects. These include the zonal rather than meridional trend of the coast, the influence of a rather narrow intense coastwise current, and an unusual lack of correspondence on the seasonal time scale between sea-temperature features attributable to upwelling, and features in the overlying wind stress field[1]. There seems to be a link between interyear variations in upwelling intensity and corresponding variations in both coastal rainfall and local fishery success.

To construct the sea-temperature distribution shown in Fig. 1, maritime reports for the period 1850–1970 were obtained from the U.S. National Climatic Center's file of marine surface observations (TDF-11), checked for gross errors, and summarised by month and by 1° 'square' areas. Mean values were contoured by hand, taking into account the abundance of observations and magnitude of standard deviations. Data abundance was greatest near the coast and to the west of Cape Palmas. The effect of warm advection in the eastward-flowing Guinea Current is apparent in the shape of the 26 °C isotherm and in the offshore temperature maximum which separates the cool temperatures along the coast east of Cape Palmas, attributable to coastal upwelling, from cool temperatures near the equator which are probably related to equatorial upwelling.

The seasonal distribution of sea-surface temperature within a line of 1° square areas stretching southward from the coast near Cape Three Points (Fig. 2) features an offshore maximum every month, suggesting continuation of some degree of coastal upwelling throughout the year. The offshore gradients are most intense from June through October; coolest coastal temperatures are reached during August and September. A secondary coastal minimum appears during January, resulting in a two-peaked annual temperature cycle.

A similar display of the seasonal cycle of sea-surface temperature (Fig. 3), this time within a line of 1° square areas arranged along the coastal boundary, reveals continuity of the summer minimum along the entire north coast of the Gulf of Guinea. In Fig. 3, west is towards the top (see Fig. 3*d*); thus the direction of flow of the Guinea Current is from the top towards the bottom of the diagram. The temperature decreases in the direction of flow to an absolute minimum east of Cape Three Points. Although the contour interval in Fig. 3 is too coarse to show it, much of the temperature decrease occurs in two abrupt steps upon passing each of the two major capes, Cape Palmas and Cape Three Points. Particularly sharp temperature gradients have been reported off Cape Palmas[2]. The coolest region, defined by the 24°C isotherm, appears in Fig. 3 to be split into two lobes by slightly higher temperatures from 0–1°W longitude; this is an artefact due to that particular 1° square being displaced slightly offshore relative to the squares to either side. Eastward of this late summer minimum feature, sea-surface temperature increases towards a region increasingly affected by outflow from the Niger River Delta and other sources. A cold temperature feature is apparent during winter in the extreme western portion of the region. The sharp gradient near 15°W longitude indicates the southern limit of the tropical front which oscillates seasonally along the west African coast between 10°N and 20°N latitudes, apparently responding to seasonal variations in wind-induced upwelling and associated along shore advection[3]. Extending eastwards from the front is a winter temperature minimum which retains its identity along the Guinea Coast well into the Bight of Biafra (~7°E longitude) where it is evident as a slight reversal during January. The two seasonal temperature minima are separated by periods of relatively warm sea-surface temperatures, with the major maximum occurring during spring.

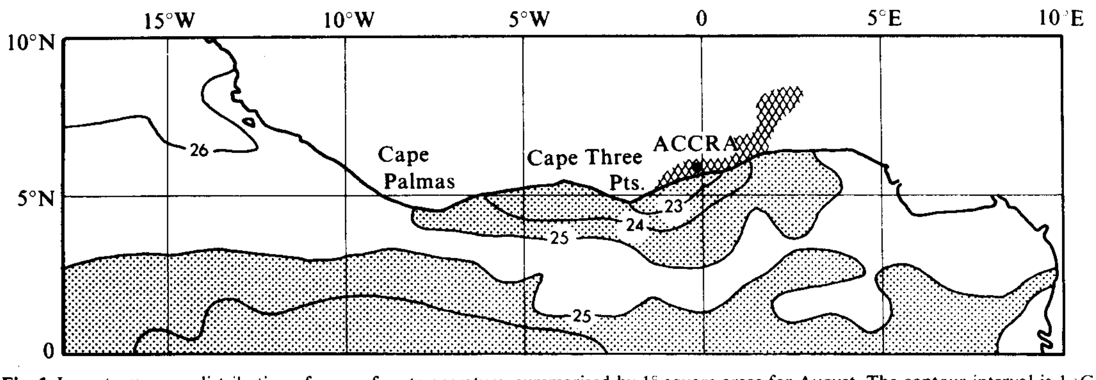

Fig. 1 Long-term mean distribution of sea-surface temperature, summarised by 1° square areas for August. The contour interval is 1 °C; temperatures less than 25 °C are shaded. The crosshatched area on the coast in the vicinity of Accra indicates an area of less than 40 inches annual rainfall, and defines the approximate extent of the Accra dry belt[16].

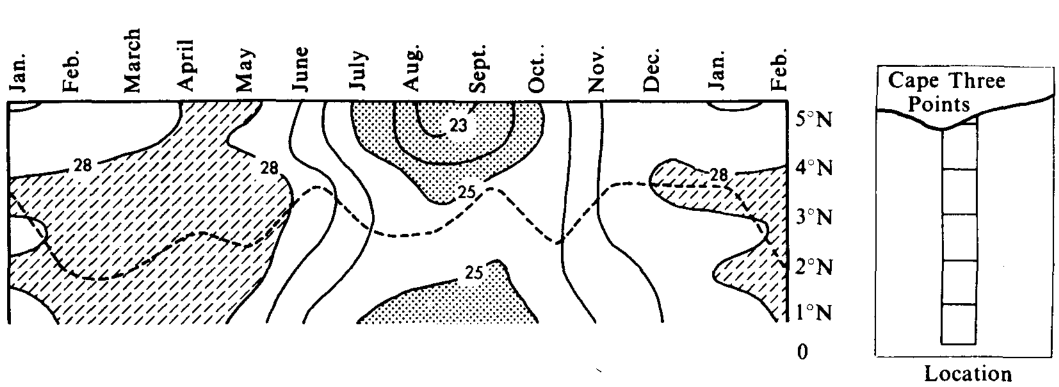

Fig. 2 Long-term composite annual cycle of sea-surface temperature within the line of 1° squares normal to the coast near Cape Three Points shown to the right. The contour interval is 1 °C; temperatures less than 25 °C are shaded, and those greater than 28 °C are indicated by broken diagonal hatching. The location of the maximum mean temperature within the line of squares for each long-term monthly sample is indicated by the dashed line.

Being near the equator, the Guinea Current region experiences two periods of vertical sun per year, one shortly before the vernal equinox and the other shortly after the autumnal equinox. Unlike the situation in more temperate latitudes, both solstices are periods of low sun. Thus, the double peaked seasonal cycle of sea temperature matches qualitatively the cycle of solar height. But compilations of mid-ocean sea-surface temperatures[4], at similar latitudes where the cycle of solar height is identical, indicate no such strong correspondence. Thus, it is difficult to ascribe the observed features directly to such large scale effects as passages of the Sun. Rather, they would seem to be almost entirely controlled by processes local to the Guinea Current region.

In the classical model for coastal upwelling[5], water set in motion by the stress of the wind is deflected offshore by the rotation of the Earth. When this occurs along an extensive stretch of coast such that the water transported off the coast cannot readily be replaced by convergence of horizontal alongshore flow, replacement can occur by upwelling of deeper water.

Previous comparisons of offshore Ekman transport distributions with corresponding temperature distributions in the California Current[6], and Canary Current[3] regions on a similar 1° scale have yielded general conformities in major features, indicating seasonal variation in the local wind as the principal factor controlling seasonality in the coastal upwelling process. Accordingly, wind reports from the Guinea Current region were assembled from the same source as the temperature reports. These were converted to measures of sea-surface stress by squaring each reported wind speed and multiplying by the density of air (assumed constant, 0.00122 g cm^{-3}) and a constant drag coefficient (0.0013). The derived stress 'reports' were then averaged by components to yield a resultant mean stress for each long term composite month and 1° square area. This was con-

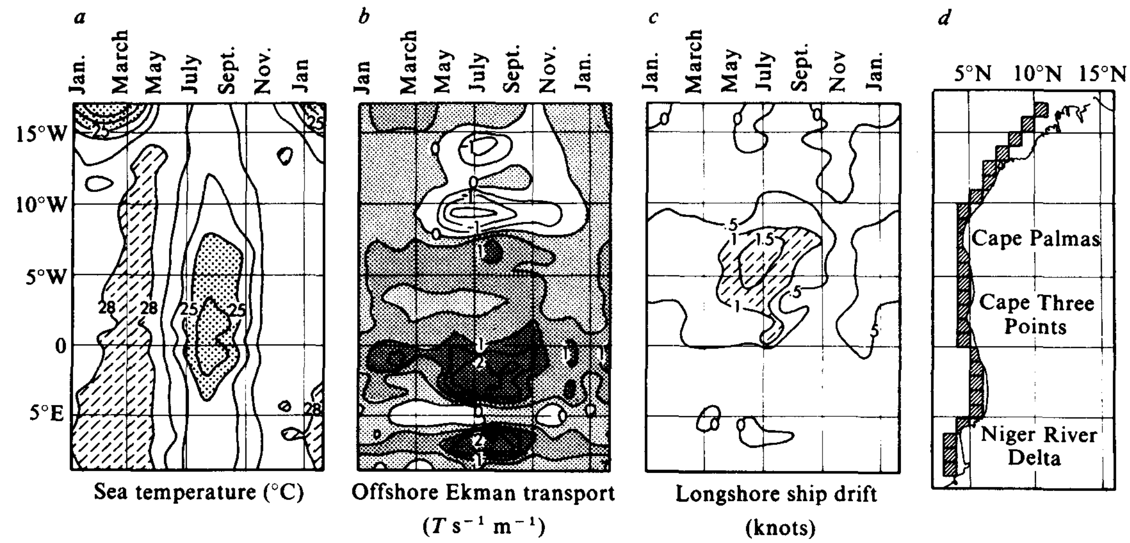

Fig. 3 Long-term composite monthly variations within the 1° square areas arranged along the coast, shown in (*d*). *a*, Sea-surface temperature. The contour interval is 1 °C; temperatures less than 25 °C are shaded and those greater than 28 °C are indicated by broken diagonal hatching. *b*, Offshore-directed component of Ekman transport. The contour interval is 0.5 tonnes S^{-1} transported across each 1 m width. Positive values, indicating seaward transport, are shaded; darker shading indicates more intense seaward transport. *c*, Alongshore component of ship drift. The positive direction is such that the coast is on the left when facing downstream. The contour interval is 0.5 knots; speeds greater than one knot are indicated by broken diagonal hatching.

verted to Ekman transport, directed 90° to the right of the stress vector, by dividing by the Coriolis parameter computed at the mid latitude of the 1° square. Where the centre of the square is less than 5° from the equator the value of the Coriolis parameter at 5°N latitude was used. Offshore components were resolved along characteristic offshore normal directions, based on the nearshore bathymetry within each individual square.

The seasonal pattern of offshore-directed Ekman transport (Fig. 3) reveals certain features which correspond to features in the temperature pattern. Transport tends to be offshore throughout the year, except during certain months off Liberia and Sierra Leone (8–14°W) and near the west-facing portion of the Niger River Delta shoreline (4–6°E). A winter maximum of offshore transport occurs in March at the northwestern end of the area (top of the diagram), and retains continuity toward the east, shifting to February off Cape Palmas and Cape Three Points. This winter maximum generally corresponds to the winter temperature minimum described above. During the summer there is a relative maximum of offshore Ekman transport on the east side of Cape Palmas and another increase to the east of Cape Three Points; these correspond to the major decreases in sea temperature near these capes.

Maximum values of offshore transport occur to the east, however, that is downstream in relation to Guinea Current observations produced as part of this study show a very significant component of the mean wind to be directed onshore at all seasons. Any larger portion of the transport being directed with the wind would, therefore, only imply a further reduction in local wind forcing of upwelling at the coast.

Figure 3c summarises reports of drift attributed to ocean currents compiled from ship's logbooks by the U.S. Naval Oceanographic Office. Although the number of available reports is very small, being of the order of 20 per month-square in the area from Cape Palmas to Cape Three Points, a coherent picture of the seasonal cycle of flow in the Guinea Current is apparent. Off Cape Palmas the current near the coast intensifies dramatically, diminishes slightly toward Cape Three Points, and drops off rapidly past Cape Three Points. Mean velocities near Cape Palmas vary from nearly 2 knots in July to less than half a knot in November. The current maximum is thus somewhat upstream of and slightly preceding the summer temperature minimum, actually coinciding in time to the period of most rapid temporal decrease of temperature and in space to the zone of most rapid spatial decrease. Horizontal advection in the current, of course, opposes the temperature decrease. Various mechanisms leading to vertical advection in an intensified current[7-10] could perhaps contribute to the observed cooling. But, the lag of at least a month between

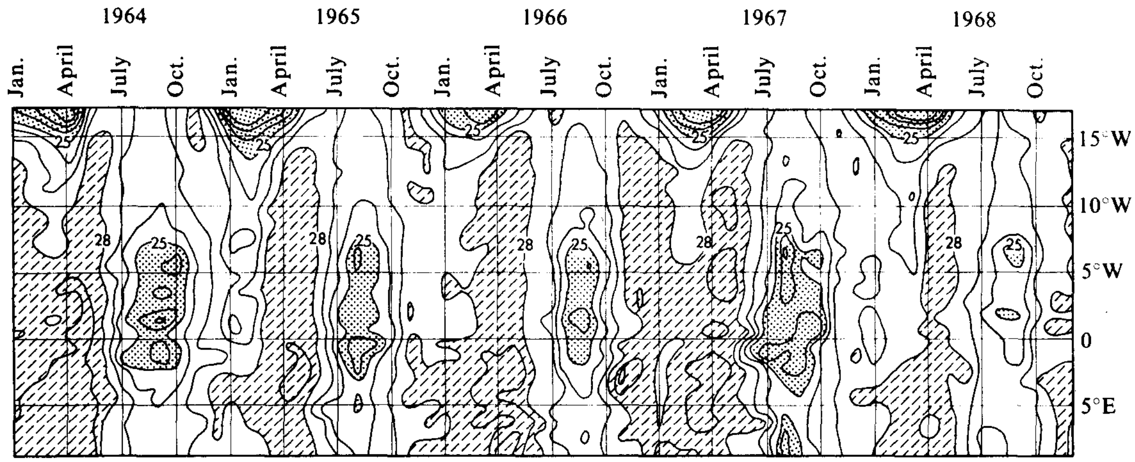

Fig. 4 Monthly temperature variation within the square areas shown in Fig. 3, during the years 1964 through 1968. The contour interval is 1 °C; temperatures less than 25 °C are shaded and those greater than 28 °C are indicated by broken diagonal hatching.

flow, of the location of summer minimum temperatures. The offshore transport maximum off Dahomey (2–4°E) is in the area of most rapid down-stream warming. Likewise, a second offshore transport maximum in the Bight of Biafra (6–9°) is not strongly reflected in the sea-temperature distribution, although both cases may involve some masking of the effects of upwelling by low salinity surface water. Certainly, there is nothing in the local Ekman transport distribution to account for the continuity of the temperature minimum to the west, that is, upstream, of Cape Palmas.

Since this region is very near the equator, the diminished Coriolis term in the dynamical equations may lead to a different balance of forces from that assumed in the Ekman transport relationship. In such a case the transport could be at a lesser angle than 90° to the direction of wind stress. Such an effect, however, cannot explain the non-correspondence of the distributions in Fig. 3. Summaries of wind the maximum current speed in July and the minimum sea-surface temperatures in August–September (Fig. 3) is difficult to reconcile with any predominant effect of such processes; for example, at the indicated average current velocities, water upwelled near Cape Palmas during the July current maximum would be carried past Cape Three Points in less than 10 days.

Recent theoretical developments have indicated the ability of upwelling-produced displacements of the internal density structure to propagate in the form of coastal trapped waves, and thus to affect the temperature and current velocity fields at other locations along the coast[11,12]. In the configuration of the Guinea Current region, the direction of propagation would be to the west. The degree of westward displacement of features in the sea temperature and drift patterns, compared to features in the Ekman transport field (Fig. 3), is consistent with computations from theory

Table 1 Comparison of intensity of summer-fall upwelling with July–October rainfall at three reporting stations in Ghana and with catch of the Ghanaian herring fishery for the years 1964 through 1968

		1964	1965	1966	1967	1968
Upwelling		High (late)	Intermediate	Intermediate	High	Low
Month		J A S O*	J A S O	J A S O	J A S O	J A S O
Rainfall (quintiles)	Accra	3 1 0 0	5 5 3 2	4 3 1 3	1 2 5 1	6 6 6 5
	Takoradi	2 4 1 0	4 4 5 1	5 4 2 2	2 2 3 1	6 6 6 5
	Kumasi	3 4 1 2	4 5 3 5	6 5 1 2	2 1 2 1	6 6 6 1
Summation		21	46	38	23	65
Herring catch (Ghana)		34.2	7.8	13.3	43.2	12.2

Upwelling intensity is estimated from sea-temperature distributions (Fig. 4). Rainfall is given in quintiles of the frequency group within which the recorded precipitation falls relative to a group of reference years[17]. 0 indicates monthly precipitation to have been lower, and a '6' indicates it to have been higher, than in any corresponding month in the reference series. In the line labelled summation the quintile values for the four months and the three stations are added together to give a seasonal index. The herring catch is in 10^3 tonnes.

*J, July; A, August; S. September; O, October.

(A. J. Clarke, personal communication). Thus it seems that such processes may be exerting particularly strong control on the pattern of seasonal upwelling in the Guinea Current.

In the surface marine observation file (TDF-11) there is an abrupt increase in the density of reports in the Guinea Current region beginning with 1964. In the particular version of the file that was used in this study, however, the frequency begins to drop off rapidly after 1968. For these five years of maximum data density a time series of sea-surface temperature (Fig. 4) was constructed on the same basis as the long-term composite annual cycle (Fig. 3). Because of the higher short-term variance of the wind, the data density was not sufficient to derive a meaningful similar series of wind or Ekman transport variations.

If one examines the summer upwelling feature (10°W–5°E longitude) in Fig. 4, it is possible to class the summers of 1964 and 1967 as having been cold (strong upwelling), 1968 as having been warm (weak upwelling), and 1965 and 1966 as having been intermediate (Table 1). In addition the strong upwelling in 1964 seems to have occurred relatively late, the coolest monthly mean temperatures appearing in September rather than in August as is the case in long-term composite cycle (Fig. 3). In partial corroboration of this classification, dissolved oxygen data collected off Ivory Coast (~4°W) during the period 1966–70[13] show low oxygen values characteristic of deeper layers unmistakably nearer the surface during the summer upwelling season of 1967 than in the other years of that particular series.

With these upwelling estimates, it is possible to look for apparent effects of upwelling variations on coastal rainfall. One mechanism which may contribute to the intense coastal aridity, which is a general characteristic of upwelling regions, is the stabilisation of the shoreward airflow by the cool upwelled surface waters, thereby inhibiting vertical development of storm clouds[14]. The Accra dry belt (Fig. 1), which has the appearance of a coastal enclave of semi-arid savanna surrounded by tropical rainforest, has been termed 'the most remarkable climatic anomaly of the Guinea coastlands'[15]. One of the unusual features cited is an anomalous dearth of rainfall during the late summer. Prevailing winds are from the south-west[16]; Figure 1 shows the Accra dry belt to be oriented directly downwind of the coldest sea-surface temperatures.

Table 1 classifies the rainfall recorded at three locations in Ghana[17]. Takoradi is located on the coast, just east of Cape Three Points. Kumasi is about 100 miles inland, between Takoradi and Accra. The correlation of the rainfall record with the upwelling estimates is convincingly strong. During the years of strong upwelling, 1964 and 1967, the July–October rainfall was anomalously low; in fact 'late' upwelling estimated for 1964 corresponds to 'late' rainfall deficits in September and October. During the weak upwelling year, 1968, monthly mean rainfall actually exceeded the highest class intervals established from historical data at all three locations during the months of July, August, and September.

Also listed in Table 1 are the landings of herring (*Sardinela aurita*) in Ghana during these same five years[18]. This was Ghana's most important fishery during this period, largely operating from canoes very near shore during the summer-fall upwelling period[19]. Evidently periods of extremely good fishing were associated with strong upwelling, as are periods of subnormal coastal rainfall. During these years a sharply increased trend in fishing effort occurred, due to technology and so on. If this is taken into account in interpreting the landing figures, a relationship is even more apparent.

ANDREW BAKUN

Pacific Environmental Group,
Southwest Fisheries Center,
National Marine Fisheries Service, NOAA, Monterey, California 93940

Received 8 July; accepted 4 November 1977.

1. Longhurst, A. R. *Bull. Inst. fr. Afr. noire* **24**, 633–633 (1962).
2. Berrit, G. R. *Cah. Oceanogr.* **14**, 719–729 (1962).
3. Wooster, W. S., Bakun, A. & McLain, D. R. *J. mar. Res.* **34**, 131–141, (1976).
4. Bohnecke, G. *Meteor* 1925-1927, **5**, 1-186 (1936).
5. Cushing, D. H. *FAO Fish. Tech. Pap.* **84**, (1969).
6. Bakun, A., McLain, D. R. & Mayo, F. V. *Fish Bull, U.S.* **72**, 843–844 (1974).
7. Hsueh, Y. & O'Brien, J. J. *J. phys. Oceanogr.* **1**, 180–186, (1971).
8. Stommel, H. & Wooster, W. S. *Proc. natn. Acad. Sci. U.S.A.* **54**, 8–13 (1965).
9. Arthur, R. R. *J. geophys. Res.* **70**, 2799–2803 (1965).
10. Ingham, M. C. *Bull. mar. Sci.* **20**, 1–34 (1970).
11. Gill, A. E. & Clarke, A. J. *Deep-sea Res.* **21**, 325–345 (1974).
12. Allen, J. S. *J. phys. Oceanogr.* **5**, 300–325 (1975).
13. Verstraete, J. M. *Doc. Scient. Centre Tech. Oceanogr. Abidjan*, **1**, 13–35 (1970).
14. Trewartha, G. T. *An Introduction to Climate* (McGraw-Hill, New York, 1968).
15. Trewartha, G. T. *The Earth's Problem Climates*, (University Wisconsin Press, Madison, 1961).
16. Steigner, J. M. & Ingham, M. C. *NOAA Tech. Rep. NMFS SSRF-643*. (US Dep. Commer., Seattle, 1971).
17. *Monthly Climatic Data for the World* **16** through **21** (US Dep. Commer., Asheville, N.C., July 1963 through Oct. 1968).
18. *Yearbook of Fishery Statistics* **26**, (Food and Agriculture Organization of the United Nations, 1969).
19. Di Palma, S. *Foreign Fisheries Leaflet* no. 77 (US Dep. Interior, Washington, D.C., 1968).

Printed in Great Britain by Henry Ling Ltd., at the Dorset Press, Dorchester, Dorset